Electron energy-loss spectra calculations and experiments as a tool for the indentification of a lamellar C3N4 compound

P. Moreau, Florent Boucher, Graziella Goglio, Denis Foy, V. Mauchamp, Guy G. Ouvrard

Electron energy-loss spectra calculations and experiments as a tool for the identification of a lamellar C_3N_4 compound

P. Moreau,[1] F. Boucher,[1] G. Goglio,[2] D. Foy,[2] V. Mauchamp,[1] and G. Ouvrard[1]
[1]*Institut des Matériaux Jean Rouxel, UMR 6502, Université de Nantes—CNRS, 2, rue de la Houssinière, 44322 Nantes Cedex, France*
[2]*Institut de Chimie de la Matière Condensée de Bordeaux, ICMCB-CNRS UPR 9048, 33608 Pessac Cedex, France*
(Received 28 September 2005; revised manuscript received 6 February 2006; published 11 May 2006)

In order to identify a poorly crystallized lamellar C_3N_4 compound using electron energy-loss spectroscopy, we first concentrate on model compounds, namely, graphite at the carbon *K* edge and hexagonal boron nitride at both *K* edges. We show that extremely good agreement can be obtained between experimental spectra and *ab initio* calculations using the WIEN2k program [P. Blaha, K. Schwarz, P. Sorantin, and S. B. Trickey, Comput. Phys. Commun. **59**, 399 (1990)]. Because the calculations are based on the density functional theory considering independent quasiparticles, they are generally believed to be inadequate to rigorously describe the excitation process. Nevertheless, we demonstrate that the spectra, when divided into two regions, above and below the ionization energy, can be simulated over a 50 eV energy range. In these materials, the first region must be simulated taking into account the electronic relaxation around a full core hole. For the second part starting usually 10–12 eV above the threshold, only a very small or no core hole at all should be introduced for the relaxation. Furthermore, we show that an empirical formula is sufficient but necessary to take into account the lifetime of the electron in the excited state. After discussion of these results on model compounds, we clearly identify the limits and benefits of these comparisons and apply them to an unknown structure. The experimental spectra were recorded at low temperature in order to avoid beam damages. They are compared with those calculated for various structures having compositions close to C_3N_4. From these core-loss studies, as well as from the corresponding low-loss ones, the structure of our sample is shown to be locally very close to that of the $(C_3N_3)_2(NH)_3$ lamellar compound described by Kawaguchi and Noziak [Chem. Mater. **7**, 257 (1995)]. This structure can also be viewed as a defective hexagonal C_3N_4 lamellar structure (with ABA stacking), rendering this compound most suitable for a further high-pressure conversion to a superhard 3D C_3N_4 phase.

DOI: 10.1103/PhysRevB.73.195111 PACS number(s): 79.20.Uv, 82.80.Pv, 71.15.Mb, 71.20.Tx

I. INTRODUCTION

In the search for new ultrahard materials, Liu and Cohen predicted,[1] using *ab initio* calculations, that the compound β-C_3N_4, isostructural to β-Si_3N_4, would present a Young's modulus as high as that of diamond. This encouraged a lot of experimental and theoretical work on CN_x compounds.[2–8] The direct synthesis of three-dimensional (3D) C_3N_4 is thermodynamically unfavored due to the high stability of N_2, even at low temperatures. A more promising outcome might result from first producing a graphitic phase via chemical vapor deposition methods[4] or via the decomposition of properly chosen reactants.[7] Then, applying pressure to the obtained compounds should lead to the formation of the superhard 3D structures.[2] In these 3D structures, the carbon atoms are tetrahedrally coordinated (sp^3 hybridization). Various sp^2 to sp^3 ratios have been obtained, revealing a rather 2D or 3D bonding character of the materials. The 3D structures present sp^3 hybridization for carbon; so the lower the sp^2 to sp^3 ratio, the better. Nevertheless, sp^2 compounds also have some interest as precursors or simply as parent compounds with valuable properties (as does graphite with respect to diamond).

A very useful technique in the determination of this sp^2 to sp^3 ratio is electron energy-loss spectroscopy (EELS) performed in a transmission electron microscope.[9] EELS allows the precise recording of the *K* edges of low-*Z* elements, in particular the electron energy-loss near-edge structures (ELNES), in the bulk and most of the time with a very high spatial resolution.[10] The ability of EELS to obtain information from very small samples is particularly valuable in the context of the production of small quantities through high-pressure synthesis or the formation of nanoclusters.[5] Top of the range experimental devices allow subnanometer spatial resolution,[11] as well as high energy resolution (0.1 eV).[12] Furthermore, diffraction and quantitative analysis are also useful tools in determining the phase actually investigated.[7,8] Going beyond the sp^2 to sp^3 ratio is crucial since Teter and Hemley,[2] predicted the existence of four phases with a pure sp^3 hybridization for carbon and also proposed many lamellar phases, with a pure sp^2 hybridization for carbon. A detailed study of the high-energy-loss spectra has to be done in order to distinguish between these phases.

Using the same general theoretical approach as Liu and Cohen,[1] i.e., the density functional theory (DFT), extended simulations of ELNES spectra are getting more and more common.[13–16] Various materials ranging from nitrides,[17,18] quantum dots,[19] nanotubes,[20,21] and even interfaces[22] have successfully been studied, and comparisons between experiments and calculations made. Numerous studies have been done on graphite, as well as on hexagonal BN but,[23–25] never with a satisfactory one-to-one comparison over the full energy range (0–50 eV), which is necessary for a complete understanding of the strengths and limitations of the techniques. Furthermore, there is no simple description of the core hole created by the ejection of the electron promoted to

levels above the Fermi level. The best approach would be to take not only the creation of this core hole into account, but also the existence of the ejected electron, the interaction between them as well as their interaction with the rest of the electrons in the material. This calculation involves the Bethe-Salpeter equation (the resolution of which remains so far the affair of specialists) which has only been applied to model compounds. If in the low-energy-loss domain some kind of expertise exists,[26] it is still largely in the development phase for core losses.[27,28] That is why material scientists currently favor ground-state calculations to compare to core-loss experiments. To simulate the core hole in that context, the Slater's transition state has gained popularity and has recently become widely used. A partial core hole can be included in the electronic structure, taking into account the variable strength interaction of the core-hole with the valence-band electrons. However, the precise strength to be used remains unclear, and an actual quantitative comparison as a function of the core-hole strength (CHS) is rarely done. Luiz *et al.*[29] clearly showed the importance of this parameter in the case of the Cu L_2 edge where they estimated the CHS to be 0.5. The same CHS was recently found satisfactory in calculating the nitrogen K edge in h-GaN but[18] a full core hole seems necessary in the case of c-GaN. The CHS should therefore be evaluated using similar structures.

We recently prepared a lamellar C_3N_4 phase of which the structure was impossible to accurately determine using diffraction or high-resolution imaging methods,[30] the reason being that this compound is poorly crystallized. ELNES is a well-known method to retrieve information on short- and medium-range atomic environments.[14,17] In order to use such a method on this new lamellar C_3N_4 compound, we found it important to first clearly assess the power of the DFT for the spectral simulations of lamellar model compounds. As a result, we now propose the arbitrary and systematic partition of the ELNES spectra into two energy domains: one below and one above the ionization energy. These domains have very different CHS values. We show that this approach gives the best agreement one can obtain with the non-time-dependent DFT.

In light of the above, this paper will be organized as follows. In Sec. II, we will carefully examine the experimental and theoretical parameters as their precise knowledge is essential for an accurate comparison. In particular, a simple and universal formula will be given which takes the broadening of the spectrum due to the finite lifetime of the ejected electron into account. In Sec. III, the carbon K edge in graphite, and the boron and nitrogen K edges in hexagonal boron nitride will be discussed. The arbitrary energy partition of the spectra will be proven to optimize simulations of the experimental results. Finally, Sec. IV will be devoted to the application of this improved description for the determination of the likely structure of our C_3N_4 compound. Identifying this phase as being closely related to the graphitic C_3N_4 structure (AB stacking) is of prime importance since it is believed to be a phase that is particularly suitable to high-pressure conversion to dense C_3N_4 structures.[2]

II. EXPERIMENTAL AND CALCULATION DETAILS

Experimental spectra were obtained with a Hitachi HF2000 transmission electron microscope equipped with a GATAN 666 EELS spectrometer and operated at 100 kV. Samples were first crushed in an agate mortar with acetone, then dispersed by ultrasound, and finally deposited onto a holey carbon grid. In order to remove any contamination, the grids, apart from the C_3N_4 sample, were heated up to 80 °C for 2 h in vacuum prior to their introduction into the microscope. C_3N_4 samples,[30] as will be shown later, are very delicate materials which undergo structural transformations (loss of nitrogen) when heated. For reference materials, the crystal orientation was carefully checked by diffraction before EELS acquisition. Both graphite and h-BN crystals were oriented with their c axis along the microscope's optical axis. The convergence and collection angles were 1.4 and 9.0 mrad, respectively. The energy resolution inferred from the full width at half maximum (FWHM) of the zero peak measured in a hole of the grid was 0.7 eV (0.85 eV for the C_3N_4 compound). A 0.1 eV/channel dispersion was used. In the case of the C_3N_4 compound, the dispersion was set to 0.2 eV/channel in order to record the C and N K edges simultaneously. The total acquisition time for each spectrum ranged from 25 to 50 s. All spectra were dark-count and photodiode-gain corrected. The spectra were deconvolved with the zero-loss peak recorded in a hole of the grid to remove the detector point spread function. An E^{-r} preedge background was subtracted from the spectra and, finally, in order to remove plural scattering effects,[31] the spectra were deconvoluted with the low-energy-loss spectrum, which was recorded on the same area. All the band structure calculations were performed using the full-potential linearized augmented-plane-wave (FLAPW) method via the WIEN2k code,[32] and within the generalized gradiant approximation.[33] A detailed description of the method can be found in Ref. 34. Muffin-tin radii were 1.34 a.u. (C) and 1.35 a.u. (B and N) for graphite and h-BN, and 1.23 a.u. for both C and N in C_3N_4 compounds. No significant changes were observed on varying any of these radii. 2s and 2p orbitals were treated as valence states using the APW+lo approach,[35] adding local orbitals (lo) to the standard APW basis and thus drastically reducing the computational time. Approximately 150 plane waves per atom were generated in the interstitial region ($R_{\min}K_{\max}=6.5$). To obtain precise total energies, self-consistency was checked over a large number of k points. Likewise, the simulated EELS spectra were obtained with a sufficient number of k points in the full Brillouin zone so that a further increase would not noticeably change the results. In the case of graphite, these k-point numbers are indicated in Table I. A common problem with linearized methods is the calculation of states far from the linearization energies, energies that are often chosen inside the valence band or close to the Fermi level. In order to accurately calculate the empty states up to 70 eV above the Fermi level, extra local orbitals (LO) were added in the s and p channels with the following linearization energies: 1.5 Ry for $l=0$ and 2.0 Ry for $l=1$. The convergence of the atomic partial density of states (DOS) with respect to those linearization energies has been checked. Core-hole calculations were obtained by removing an electron, or a fraction of an electron, from the 1s level and adding the corresponding charge as a background charge for global neutrality. To reduce interactions between two neighboring core holes, supercells were used with either two, four,

TABLE I. Parameters, total energies, and transition energies for different supercells used in the calculation of graphite ELNES spectra. $\Delta_{SCF}=(E_{total}-E_{no\ hole})$ (Nb atoms/cell). BZ indicates the Brillouin zone.

Type of unit cell	Number of atoms in the unit cell	k points for SCF cycle	k points in full BZ for ELNES	E total (eV/atom)	Δ_{SCF} for transition (eV)
No hole	4	400	3388	−1036.8515	
Core hole $a\times a$	4	340	3388	−965.18967	286.65
Core hole $2a\times 2a$	16	75	1156	−1018.9860	285.85
Core hole $3a\times 3a$	36	48	648	−1028.9144	285.74
Core hole $4a\times 4a$	64	28	252	−1032.3868	285.74

six, or eight atomic bonds separating each core hole (see Table I).

EELS spectra were simulated using the built-in ELNES program of the WIEN code.[13] The doubly differential cross section for inelastic electron scattering was evaluated taking up to octopole transitions into account. Hébert *et al.*[13] showed that due to orthogonalization errors between the empty states and the 1*s* core states, and mainly for light elements, monopole transitions were not nil. These transitions having no physical meaning, $\Delta l=0$ transitions were always removed to get the final theoretical spectrum. The main intensity of this monopole contribution is situated between 10 and 15 eV above threshold, where the 3*s* character of the wave function is strong. Results for low CHS values showed small monopole contributions (less than 5% of the main dipole intensity) in the C and N edges, and much larger ones in the boron *K*-edge simulation. In the case of large CHS values, the monopole contribution is negligible for all elements, illustrating the contraction of the 1*s* level. Its smaller extension outside the muffin-tin sphere reduces the orthogonalization problem with the *p* levels.

An accurate portrayal of the experimental intensities implies the appropriate description of the finite lifetimes of the core hole and of the ejected electron. As regards the light elements involved in this paper, the Lorentzian broadening due to the core hole is extremely small and was therefore set to 0.1 eV as extrapolated from lifetime broadening tables. We also included the lifetime of the electron in the excited state, which is often not taken into account in DFT literature but is very common in multiple-scattering programs like FEFF.[36] We then chose to use the universal curve describing the inelastic mean free path of the ejected electron as a function of its kinetic energy.[37] In a log-log plot, we approximated this curve to be two straight lines. Making use of Heisenberg's uncertainty principle, we found the following energy-dependent Lorentzian broadening parameter (in eV):

$$\Gamma(E)=0.3906\left(\frac{123}{(E-E_0)^{2.43}}+0.056\right)^{-1},$$

for $E>E_0$. For $E\leqslant E_0$, the broadening due to the lifetime of the electron in the excited state was considered to be negligible. $E-E_0$ represents the kinetic energy of the ejected electron with E_0 the ionization energy at the edge considered. Although this E_0 parameter depends on the material studied, the resulting spectra do not rely on its exact value (within 2–3 eV). It was set to 9 eV for both atoms in *h*-BN, 5 eV for C in graphite, and 7 eV for both atoms in our C_3N_4 sample, based on best agreement with experimental spectra. This reference energy plays the same role as the reference energy E_0 fitted in extended x-ray absorption fine structure studies, which usually lies in the main intensity rise after the edge. This method is equivalent to the one used by Le Bossé *et al.*[16] but with the advantage of requiring only one free parameter (E_0). The calculated spectra were then convoluted by a 0.7 eV (0.85 eV for the C_3N_4 compound) Gaussian to account for the experimental resolution.

In the case of the structure named ZZ in Sec. III, the detailed atomic positions were not available in literature. Consequently, for this structure only, the cell parameters and atomic positions were optimized using the VASP code by minimizing Hellmann-Feynman forces.[38] This package is based on an efficient and accurate projected augmented wave approach.[39,40] The Perdew-Burke-Ernzerhof 1996 functional was used for the exchange and correlation potential.[41] The convergence of the total energy with respect to the size of the basis set and the **k**-point density has been checked. We used an energy cutoff of 500 eV and a $3\times3\times4$ Monkhorst-Pack **k**-point mesh.

III. RESULTS ON MODEL COMPOUNDS

A. Carbon *K* edge in graphite

Before starting the EELS investigations on the C_3N_4 compound, we will show by studying model compounds like graphite and *h*-BN how EELS simulation can be improved. Notably, a variable core-hole effect was introduced into the simulation. The carbon *K*-edge experimental spectrum of graphite is presented in Fig. 1 and is very similar to previously published results.[42–44,24] The positions of the π^* peak (labeled 1) and higher-energy peaks are in perfect agreement with those given by Wibbelt *et al.*[44]

The DOS convergence is particularly difficult to attain and over 3000 *k* points in the full Brillouin zone were necessary. Whereas simulated spectra did not vary much in the 0–10 eV and 15–40 eV areas above threshold, the intensity calculated in the 10–15 eV region was particularly sensitive to the number of *k* points.

Table I gathers all the relevant parameters used in the carbon *K*-edge simulation. Since two crystallographically different carbon atoms exist in graphite (C1 at 0,0,0 and C2

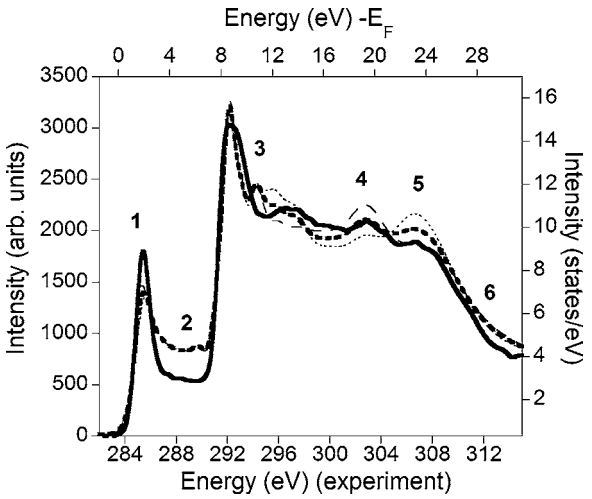

FIG. 1. Comparison of experimental carbon *K* edge in graphite (thick line) with the calculated ground-state ELNES (thick dashed line). The calculated spectra for the two inequivalent carbons are also presented (thin dashed and dotted lines). Labels 1–6 mark areas discussed in the text.

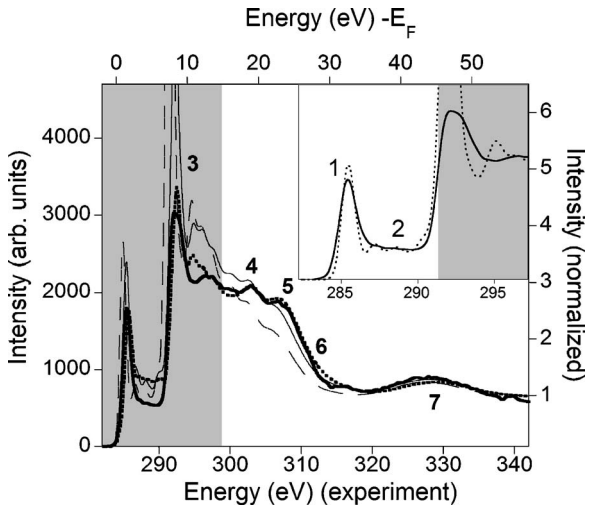

FIG. 2. Comparison of experimental carbon *K* edge in graphite (thick line) with ELNES spectra calculated using different core-hole strengths. CHS 0.1 in a $2a \times 2a$ supercell (thick dashed line); CHS 0.5 in a $4a \times 4a$ supercell (thin line); CHS 1 in a $4a \times 4a$ supercell (long dashed line). Both inequivalent carbon atom contributions were added. Inset: comparison of experiment (thick line) and CHS 1 calculation (dotted line) in the π^* region. Labels 1–7 are discussed in the text. Gray areas indicate energy ranges where the correspondence between experiment and calculations is expected to be poor and illustrate the energy range partition discussed in the text.

at 1/3,2/3,0), each contribution is presented in Fig. 1. While both spectra are very similar at low energy, some differences are clearly seen at around 20 eV above threshold. In particular, whereas the peak at 303 eV (labeled 4) is mainly due to the C1 atom, the peak at 306 eV (label 5) is mainly related to C2. This shows that this energy region is very sensitive to the stacking of the graphene layers and this sensitivity will later be used in our study of the C_3N_4 sample. In this energy range, the inelastic mean free path of the ejected electron is relatively large (the so-called multiple-scattering region) and information can be obtained on second or third neighbors. From 0 to 10 eV above threshold (labels 1 and 2), on the other hand, the empty electronic levels are very localized (molecularlike) and mainly related to the C1 and C2 atom's nearest neighbors, which are identical. Likewise, the position of the first extended energy loss fine structure (EXELFS) oscillation, at around 328 eV (not shown), is identical for both carbon atoms. Indeed, the inelastic mean free path of the ejected electron gets small after 40–50 eV,[37] and the spectra become essentially characteristic of the first coordination shell around the considered atom. Adding up both contributions, general agreement between calculation and experiment is reasonably good but could still be improved on some points.

(i) The calculated π^* peak (label 1 in Fig. 1) is too small and too broad (FWHM 1.9 eV instead of 1.4 eV experimentally). Regarding the π^* peak width, a detailed study by Ahuja *et al.*[23] was performed by comparing full-potential linear muffin-tin-orbitals (FPLMTO) calculations and x-ray absorption spectroscopy (XAS) experiments. The core-hole effects were shown to have been responsible for this width discrepancy as well as for its incorrect positioning with respect to the Fermi level (2 eV above instead of 1 eV as experimentally observed). This paper did not, however, discuss the peak's intensity with respect to the rest of the spectrum. This intensity is very sensitive to the knowledge of the scattering conditions in the microscope, which we took great care to monitor precisely. (ii) The intensity around label 2 is also wrong by almost a factor of 2. (iii) The region around label 3 is badly reproduced. (iv) The intensity of the peak at label 5 is slightly too large. (v) The width of the σ^* band is also slightly too large (label 6).

As already done by many authors, a full or partial core hole was introduced and a supercell considered to avoid interaction between core holes. To allow a better comparison, all simulated spectra in Fig. 2 were normalized at 57 eV. In the case of a full core hole and a 0.5 core hole, the interaction between holes is so strong that $4a \times 4a$ supercells were necessary in agreement with Ahuja *et al.*[23] Usually, five bond lengths have to separate full core holes to avoid any interaction. But for partial 0.1 CHS, a $2a \times 2a$ supercell was used and proved to be enough. The introduction of a 0.1 CHS slightly improves the agreement on the width of the σ^* band (label 6) and renders this simulation almost indistinguishable from the experiment from 297 eV onward. Larger CHSs have a very detrimental effect on the intensity (labels 4–6), which precludes the utilization of a full core hole to describe the ELNES spectra in the 10–30 eV above threshold region. However, let us note that the first EXELFS oscillation at 328 eV (label 7) is correctly positioned, whatever the CHS. Actually, what is most significant is the energy difference between this peak and the intensity rise (the edge "jump" around 291 eV) as established by the "Natoli rule."[45] The energy difference is found to be 38 eV (±0.2 eV depending on the CHS), which corresponds well with the 37±0.5 eV of the experiment. There is consequently a slight overestimation (2.6%).

If from 10 eV above threshold the full core hole degrades the simulation, such is not the case below this energy. In

truth, the intensity, as observed around the labels 1 and 2 in the inset of Fig. 2, is almost perfectly reproduced. The full width at half maximum of the π^* peak is then 1.1 eV and is now smaller than the experimental width. Ahuja *et al.*[23] explained this discrepancy by a vibrational broadening (0.5 eV) which is not included in our calculation. In the case of a full core hole, the π^* peak appears 0.95 eV above the Fermi level. Since the 1*s* binding energy in x-ray photoemission spectroscopy (XPS) experiments is 284.4 eV with respect to the Fermi level,[46] the calculated position of the π^* peak (0.95 eV above this value) is in perfect agreement with the experimental position (285.4±0.2 eV). Smaller CHSs place the π^* peak way too high above the Fermi level (1.5–2 eV above E_F).

The region of label 3 cannot be fitted whatever the core-hole strength. Since monopole transitions are found to be negligible in this carbon *K*-edge case, the reason for this discrepancy should be sought in the intrinsic limitations of the method.

There is a long-standing controversy over the "magic angle" in EELS; in other words a combination of convergence and collection angles that would allow the collection of orientation-independent spectra for crystalline materials. Most studies are based on the comparison of the experimental and theoretical carbon *K* edge in graphite.[47–49] From our calculations, it is clear that the formulas used in the TELNES program[25] correspond well with experiment if one treats the low-energy part with a CHS of 1 and the high-energy part with a CHS of 0.1. Since the π^* peak lies in the low-energy region and the σ^* bands in the high one, some incompatibility exists which might prevent the accurate determination of the sp^2 to sp^3 ratio and explain at least part of the experimental and theoretical discrepancies.[49,50]

Finally, it should be noted that we did not obtain a broad peak between the π^* and the σ^* bands, the so-called interlayer states.[51–54] This peak was found either when the interaction between core holes was sizable, i.e., when the supercell was too small (a $2a \times 2a$ cell, for example), or when the *k*-point mesh was too small. In fact, its experimental observation can be linked to the spectral contribution of C-H* bonds at the surface of graphite.[55]

To test our partition of the spectrum into a full core-hole region (at low energy) and a weak CHS region (at high energy), it was important to perform the same study on another model compound with, for example, a large band gap to assess its influence on the simulations. The relevant results on *h*-BN are presented in the following section.

B. Boron and nitrogen *K* edges in *h*-BN

Experimental B and N *K* edges are presented in Figs. 3 and 4. They are in exact accordance with XAS measurements from Franke *et al.*[56] At the boron *K* edge, the peaks labeled from 1 to 5 are, in this experiment, at 191.9, 198.1, 204.0, 207.4, and 215 eV, respectively (±0.2 eV). All these values lie within 0.2 eV of the XAS values. At the nitrogen *K* edge, the peaks labeled from 1 to 5 are at 401.6, 408.1, 415.4, 427, and 440.5 eV, respectively (±0.2 eV). All these values lie within 0.2 eV of the XAS values, apart from the last three

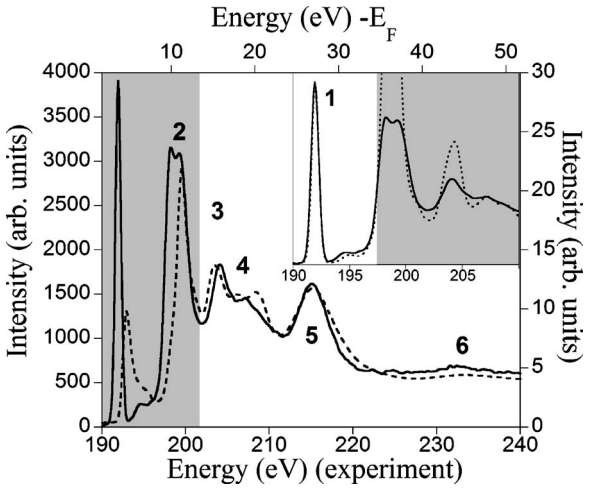

FIG. 3. Comparison of experimental boron *K* edge in *h*-BN (full line) with ELNES spectrum calculated using CHS 0.1 (dashed line). Inset: comparison of experiment and CHS 1 calculation in the π^* region.

which are 0.5 eV lower in energy in this study. Considering the width and intensity of these peaks, such a difference is not significant.

As regards the calculations, one must first note that the two inequivalent boron sites (as well as nitrogen) have identical ELNES spectra and that one can limit calculation time by focusing on one particular atomic site for N and one for B. With respect to the high-energy side (from 10 eV above threshold), our calculations correspond well with experimental spectra, for both edges, when a 0.1 CHS is introduced (Figs. 3 and 4). In this case, the calculated intensities as well as peak positions are within the error of the experiments. However, other CHSs do not change the spectra as much as in the case of graphite, and 0.1 for the CHS should not be taken as a very precise value (0.2 or no core hole are almost as good). The agreement at the boron *K* edge, around

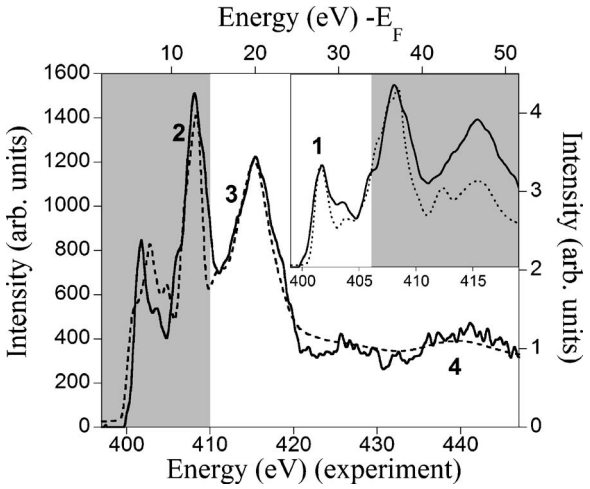

FIG. 4. Comparison of experimental nitrogen *K* edge in *h*-BN (full line) with ELNES spectrum calculated using CHS 0.1 (dashed line). Inset: comparison of experiment and CHS 1 calculation in the π^* region.

199 eV, is not very satisfactory which is rather unexpected if one considers the perfect agreement obtained at the nitrogen *K* edge in this energy region. Simulations for the low-energy part of the experimental spectra are presented in the insets of Figs. 3 and 4. Once again, with the full core hole, there is a very good agreement between our calculations and our experiments, in the 0–7 energy range above threshold for both edges.

At the boron *K* edge, the first EXELFS oscillation is calculated 33.3 ± 0.2 eV above E_0 (34.5 ± 0.5 eV experimentally) and, at the nitrogen *K* edge, it is calculated 35.2 ± 0.2 eV above E_0 (36.0 ± 0.5 eV experimentally). There is in this case a slight underestimation of the energy position of the first EXELFS oscillation. Considering the overestimation in the case of graphite, we can assume a 2% error on this oscillation position. This is most likely due to the error made in the determination of E_0 on both theoretical and experimental spectra. Still, this implies that we can be fairly confident about the first-coordination-shell distance inferred from the simulation, and may use it as a structural characteristic.

C. Discussion concerning the model compound results

In the context of lamellar structures and light elements, we showed that a very small CHS (0 or 0.1) must be used to interpret the high-energy part of the spectrum, whereas a large core hole (close to 1) must be introduced to simulate the low-energy one. The boundary between the two energy regions is situated approximately around the main intensity rise in the spectra, i.e., around the ionization energy E_0. This arbitrary partition does not seem to be linked to either the DFT or the kind of computational program. The same conclusions could in fact be drawn from the examination of simulations obtained using the multiple-scattering program FEFF8.[36] With this program, as expected, the use of a full core hole is definitely a more effective way of matching the edge onset in the experimental boron *K* edge of cubic BN.[57] As for the high-energy part of the spectrum, the calculation without a core hole seems a better match (ground-state calculation of Fig. 1 in Ref. 57, peak at 205 eV) when normalized far from the edge. However, further investigation is clearly necessary in order to assess to what extent the proposed arbitrary partition depends on the calculation method.

To justify such a partition from a physical point of view, one could suggest that it is based on the different lifetimes of the excited states. For energies below or close to E_0, the lifetime is rather long. Based on the inelastic mean free path values,[37] it can be estimated of the order of 5×10^{-15} s. The rather large value of this lifetime is to be expected when considering, for example, the very small full width at half maximum of the π^* peak (hardly any "lifetime broadening") and the sharpness of excitonic peaks in diamond and graphite.[58] For energies starting at 20–30 eV above E_0, the inelastic mean free path gets smaller (2 nm) as does the lifetime of the excited state. This can also be estimated and found in the order of 1.5×10^{-17} s. If we then use the full width at half maximum of the plasmon as an indication of the relaxation time of the valence electrons in a compound,[15] we find the value of 6×10^{-17} s for graphite. Consequently, for energies high above E_0, the valence electrons do not have time to relax due to the presence of the core hole before the transition is completed. This leads to the so-called sudden approximation. For energies below or close to E_0, the valence electrons relax before the end of the transition. This produces large core-hole effects, and a self-consistent calculation with a core hole is necessary. We expect this partition to be very dependent on the relaxation time of the valence electrons and therefore on the metallic or insulating nature of the material considered.

Aside from this, when large kinetic energies of the ejected electron are considered (starting from ~50 eV above E_0), simulations with and without a core hole become very similar, the only difference being a small energy shift. The explanation for this may be that the larger the ejected electron kinetic energy is, the lower its sensitivity to the variation of the electronic density around the excited atom.

Finally, as pointed out by Hamman and Muller,[59] the use of two such calculations is a technical way of solving a simulation problem. Solely the resolution of the Bethe-Salpeter equation accounts for the entire spectrum intensities, particularly in the region of E_0. One should also bear in mind that calculations that include a core hole do not incorporate excitonic effects as such, since the calculations are monoelectronic and the interaction of the core hole with the ejected electron is not included. Having established the theoretical limits and the practical benefits of the above study, the following section will deal with its application to the structural identification of a poorly crystalline C_3N_4 compound.

IV. RESULTS ON THE C_3N_4 COMPOUND

First of all, we must stress how sensitive our sample is to the electron beam, as is probably the case with most CN_x compounds. With respect to room temperature experiments, the C to N ratio determined from the *K*-edge intensities was systematically too large: around 3 ($\pm 10\%$). Even at liquid nitrogen temperature, the ratio was not lower than 1.5 when the probe was focused on a few nanometers. Only when liquid nitrogen temperature was combined with a large probed area (above 500 nm) were C to N ratios found equal to 0.78. Due to the inhomogeneity of thickness over such large sampled areas, edge count extractions and the common uncertainty on calculated cross sections, the error on the C to N ratio is around 10%. Even with such experimental care, the low-energy part of the ELNES appears to be extremely sensitive to the radiation damage, without a significant evolution of the atomic ratio value. If the beam is left at the same position and successive spectra are recorded, a dramatic change is observed on both C and N edges, as illustrated in Fig. 5. The multiple-scattering region (from 10 to 40 eV above threshold) is also affected with a softening of the spectra toward edge shapes found in the case of fully amorphous compounds. Meanwhile, the C to N ratio increases slightly but stays with in the 10% error bar (from 0.78 to 0.84). However, whereas the carbon edge presents a new peak at lower energy, in agreement with its reduction following the departure of nitrogen, the nitrogen *K* edge be-

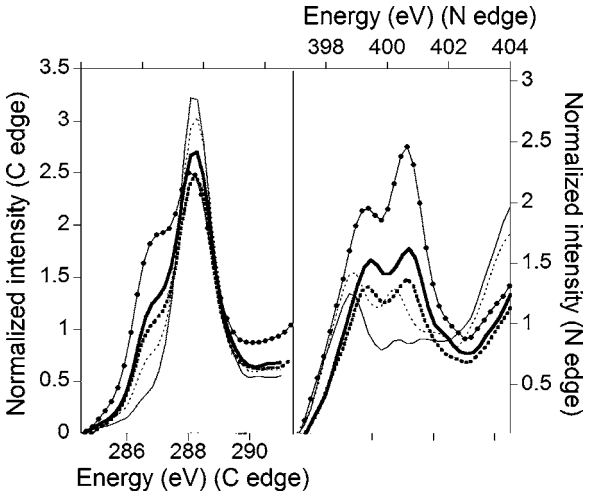

FIG. 5. Evolution of the carbon *K* edge (left) and nitrogen *K* edge (right) as a function of time in our C_3N_4 sample. Spectra are recorded on the same area for 10 s every 10 s in the following order: thin line, thin dashed line, thick dashed line, thick line, line with dots.

haves more hieratically. This illustrates the careful consideration required in the assessment of radiation damage in CN_x compounds.[5] Considering the large peak at low energy on the carbon *K* edge, it is obvious that the synthesized compound is lamellar. From the C to N ratio, a lamellar C_3N_4 structure, or close to C_3N_4, is expected. Many studies of such lamellar structures have been published and we decided to check on which one was closest to ours. The three selected in-plane structural arrangements are presented in Fig. 6, labeled (a) to (c). For the first in-plane arrangement [Fig. 6(a)], we considered two stackings *AA* or *AB*. Structural parameters were

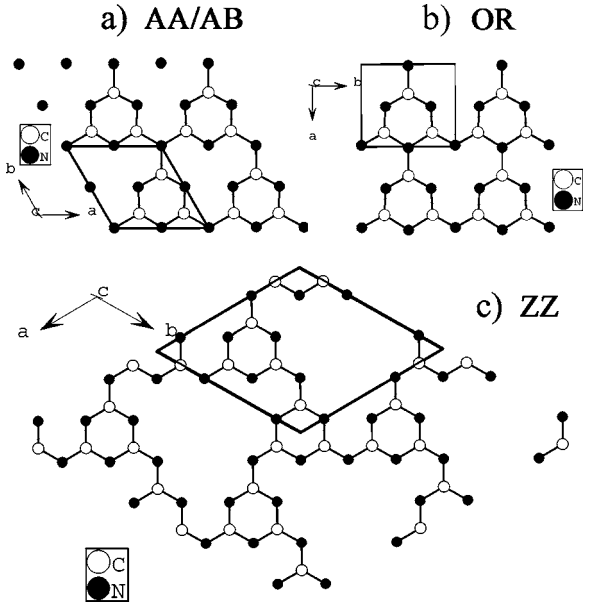

FIG. 6. The three in-plane structures used for the simulations of ELNES spectra. (a) Hexagonal structure from Ref. 3. Two stackings are considered in the text, *AAA* and *ABA*. (b) Orthorhombic structure from Ref. 60. (c) Hexagonal structure from our optimization.

TABLE II. Cell and atomic parameters obtained for the *ZZ* structure after the geometry optimization performed using the VASP program. Space group $P63/m$ (no. 176).

Cell parameters (Å)	Atomic positions
$a=8.6292$	C1 (0.50245, 0.20315, 3/4)
$c=6.8131$	C2 (0.96565, 0.12999, 3/4)
	N1 (0.52626, 0.36798, 3/4)
	N2 (0.94502, 0.27833, 3/4)
	N3 (0.03491, 0.85982, 3/4)

taken from Mattesini *et al.* for these two phases.[3] The orthorhombic phase [OR, Fig. 6(b)] was also taken from Ref. 3 following the original work of Alves *et al.*[60] Since the *ZZ* structure [Fig. 6(c)] was not published with defined cell and atomic parameters,[7] we optimized the structure using the VASP code. The structural parameters are gathered in Table II. In fact, the *ZZ* structure refers to a composition with a C to N ratio equal to 0.67, which is lower than the EELS experimental value but is closer to the standard chemical analysis result.[30] The three bridging nitrogen atoms are hydrogenated, leading to an electronic structure very similar to that of C_3N_4. The in-plane arrangement of the C and N atoms in the *ZZ* structure can be obtained from the *AA* one by simply removing one C_3N_3 ring out of three. Unfortunately, the introduction of hydrogen atoms in the WIEN calculation is very computer demanding and not feasible in practice. Consequently, we artificially added three electrons per formula unit to the total number of electrons and compensated for them by a positive background charge. Later it will be shown that, while this method is not suitable for the determination of the transition energy, it is acceptable for the spectrum simulations.

Due to our interest in the structural information contained in the multiple-scattering region, and based on our previous results showing satisfactory agreement on model N and C *K* edges for a very low CHS in this region, we present calculations with no core hole for the four structures considered. Owing to the non crystalline nature of the material, no specific orientation could be evidenced. Consequently, for each structure and each atom, three spectra corresponding to the three orientations (momentum transfer along *a*, *b*, or *c*) were added. Due to the average convergence and collection angles, the ELNES spectra do not vary much as a function of orientation.[47]

The spectra for the four structures are very different. An interesting feature in the experimental spectrum shown in Fig. 7 is the steplike structure around 307 eV which is very unusual, and is consequently characteristic (label 3 in Fig. 7). Two such structures among those calculated presenting such a feature at the right energy position are the *AB* and the *ZZ* ones (Fig. 7). Other peaks are also found at approximately the proper energy. Other calculations using an *ABC* stacking (not shown) do not present a significant difference with the *AB* stacking results. The local environment of the carbon atoms differs only at large distances between *AB* and *ABC* structures, whereas the second coordination shell is already different for *AA* and *AB* stackings.

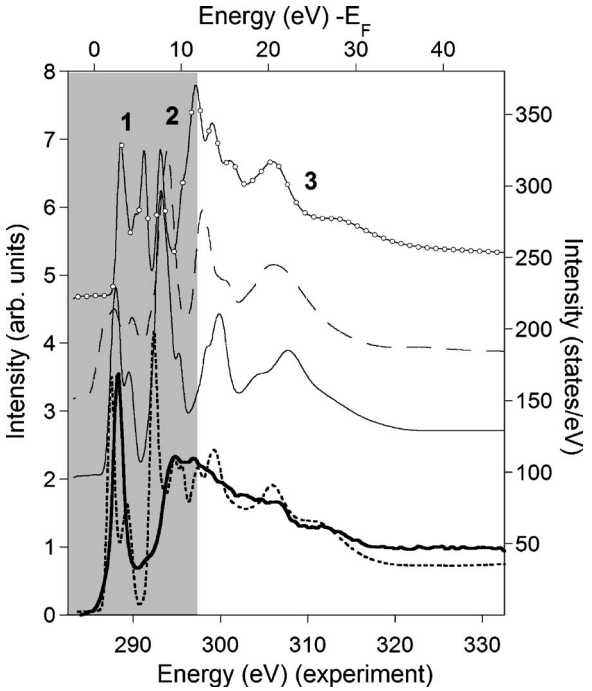

FIG. 7. Comparison of the experimental carbon *K* edge of our sample (thick line) with calculated ones using different structures: *AB* (thick dashed line); *AA* (thin line); OR (long dashed line); and *ZZ* (line with empty circles).

If the second part of the ELNES spectrum fits well, the first part does not, in either the *AB* or the *ZZ* structure. In particular, instead of a single one, two π^* peaks are calculated (label 1 in Fig. 7) originating from the carbon *p* contribution into the *p* levels of the N1 (in the C_3N_3 ring) and N2 atoms (bridging) respectively.[3] In order to correctly simulate the first part of the carbon *K* edge, a core hole in a $2a \times 2a$ supercell was introduced into the *AB* structure. The *ZZ* cell being large enough, the core hole was introduced into the structure without any increase in the size of the unit cell. Both these simulations have a drastic effect on the resulting spectra since a single peak is then obtained, the intensity and width of which are in reasonable agreement with those of the experiment (Fig. 8). A few eV above this single π^* peak, however, the spectrum shapes differ. As per the previous calculation on graphite and boron nitride, the agreement is expected to be good up to 6 eV after the π^* peak. From Fig. 8, it is clear that the *AB* structure presents a peak at 293 eV which is too intense and situated too high in energy. On the contrary, the *ZZ* structure fits the experimental spectrum rather well in this energy range (label 2 in Fig. 8). To confirm any assignment, the agreement must also be good at the nitrogen *K* edge. In the ground-state calculation, in adding up all inequivalent nitrogen contributions (N1 and N2), a very good correspondence can be observed for the second part of the ELNES spectrum between the experimental spectrum and both *AB* and *ZZ* structures (Fig. 9). From that part of the spectrum, it is once again very difficult to choose between the two structures. To simulate the first part of the spectrum, core holes were introduced in an *AB* $2a \times 2a$ supercell and a *ZZ* structure. Since only the sum of both N1 and N2 contributions is measured by EELS, one is faced with the delicate task of adding up N1 and N2 spectra obtained from two independent DFT calculations. In the case of the *AB* structure, N1 and N2 transition energies are separated by 2.2 eV (energy difference between the 1*s* levels of the two nitrogen atoms), in agreement with the Mattesini *et al.* calculations.[3] In the case of the *ZZ* structure, a 0.8 eV separation is found (to be discussed in the next section). We chose to use these values to shift the π^* peaks accordingly, i.e., a 2.2 eV separation between N1 and N2 atoms for the *AB* structure and a 0.8 eV separation between N1 and N2 atoms for the *ZZ* structure. The theoretical spectra were then added and convoluted by a Gaussian function (FWHM 1.2 eV) to account for the poor crystallinity of the sample. The agreement is

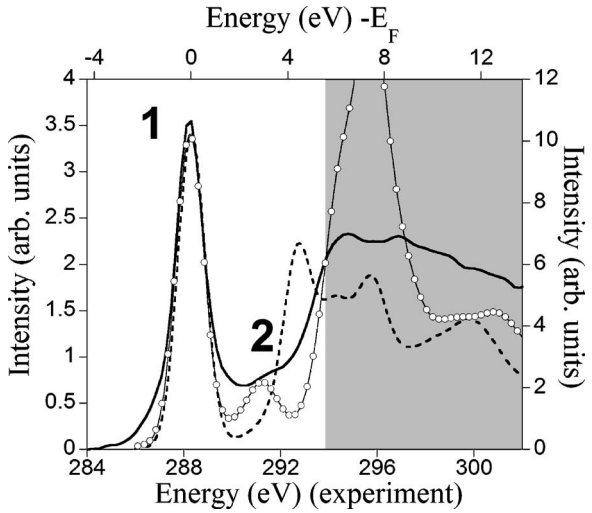

FIG. 8. Comparison of the experimental carbon *K* edge of our sample (thick line) with the *AB* structure calculation for CHS 1 (dashed line) and the *ZZ* structure calculation for CHS 1 (line with empty circles).

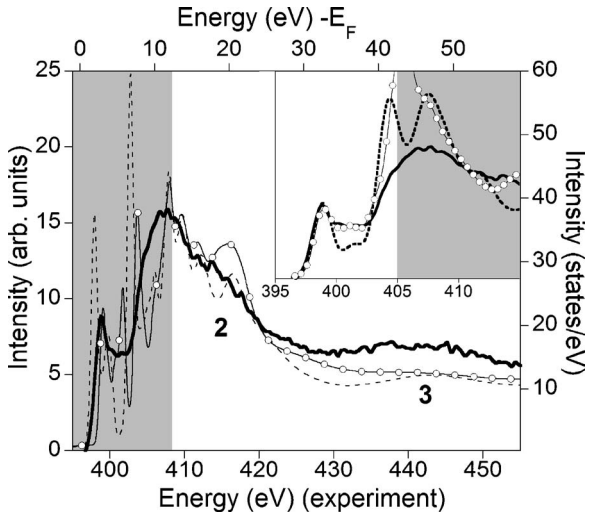

FIG. 9. Comparison of the experimental nitrogen *K* edge obtained for our sample (thick line) with the *AB* calculation (dashed line) and the *ZZ* calculation (line with empty circles). Inset: comparison of the experimental nitrogen *K* edge obtained for our sample (thick line) with the calculations for CHS 1.

once again reasonably good for both structures, with a perfect fit over the first 5 eV for the *ZZ* structure (Fig. 9, inset). It should be noted that the intensity discrepancy observed 10 eV above the π^* peak is meaningless (as in the graphite case, Fig. 2) and constitutes the main limitation of non-time-dependent calculations.

From ELNES simulations, the attribution to either the *ZZ* structure or the *AB* nanocrystalline one seems to be evident. Edge energy positions as well as π^* peak positions are also often used to identify compounds. Since these energies can be assessed theoretically using DFT, let us discuss some of our results concerning this issue. Transition energies corresponding to the promotion of a single 1*s* electron to levels above the Fermi level may be obtained from the difference Δ_{SCF} between the total energy of a ground-state calculation and the total energy of the same structure with a core hole.[15] The generated supercells, which must be sufficiently large to avoid core-hole interaction, are illustrated in the case of graphite by the larger transition energy found with a $2a \times 2a$ supercell with respect to a $4a \times 4a$ supercell (Table I). Such an evolution is also indicative of how large the supercell must be in order to obtain a proper ELNES simulation. All our calculations confirm the results found by Ahuja *et al.*,[23] stating that a minimum of four bonds must separate two core holes in the structure. An alternative method of estimating the transition energies is to introduce a 0.5 hole in the 1*s* level and then to ascertain the energy of this 1*s* level after running the self-consistent cycle (using Slater's transition state theory).[61] Energies are systematically lower using the 0.5 hole than with the Δ_{SCF} method and, depending on the compound, the energy difference between the two methods can also vary up to 1 eV. This illustrates the susceptibility of the methods to the structure, and consequently the degree of imprecision one can expect in the determination of the absolute energy transitions. Similar tendencies can be found from results on the *AB* and *ZZ* structures. For example, calculations for the *ZZ* structure do not give realistic values. The carbon transition energy in this structure, Δ_{SCF}, is equal to 291.5 eV, a 3 eV shift from the *AB* value (288.7 eV). We should recall that in order to perform the calculation for the *ZZ* structure with the WIEN2K package, three electrons have been introduced by artificial means (to simulate the three hydrogen atoms) and then compensated for using a positive background charge. Furthermore, introducing a core hole also imposed the addition of yet another electron as a background charge. This proves to be too great a manipulation for the reasonable determination of the absolute transition energies in the *ZZ* structure. This is confirmed when one performs such a calculation on a hypothetical $Li_{1.5}C_3N_{4.5}$ structure, identical to the *ZZ* one with Li atoms in place of hydrogen ones. The idea behind the artificial use of lithium atoms is to avoid the introduction of too many extra electrons by hand. In using lithium atoms, Δ_{SCF} transition energies for the *ZZ* structure (289.1, 400.8, and 401.6 eV for C, N2, and N1, respectively) become very similar to those of the *AB* structure (288.7, 400.6, and 402.8 eV for C, N2, and N1, respectively).

Due to all these uncertainties, the absolute values should be compared with experiment very carefully. Even if most Δ_{SCF} or transition-state energies agree quite well with the experimental values, in particular at the carbon *K* edge, the absolute precision (1–2 eV depending on the edge and the method considered) is not sufficient to discriminate safely between, in fact, very similar C_3N_4 structures. These findings are consistent with the results of Paxton *et al.* who had to introduce a 4.2 eV downward shift to fit the experimental C and N threshold energies in some nitrides and carbides,[15] and with Hamann and Muller's conclusions that using DFT, the accuracy of the absolute energy determination is not better than 1 eV.[59]

However, within a given structure, energy shifts from one nitrogen atom to another should be more reliable. That is the reason why a 0.8 eV (2.2 eV) energy difference between N1 and N2 atoms in the *ZZ* (*AB*) structure was used in the simulations presented in the inset of Fig. 9.

V. LOW-ELECTRON ENERGY-LOSS SPECTRA

A final point in favor of this attribution to a *ZZ* structure or a highly defective *AB* structure, lies in another energy region available in EELS: that of the low energy loss. From the same band structure calculations we used for the ELNES area, it is possible to produce spectra for losses between 0 and 50 eV. The complete dielectric function (ϵ_1, ϵ_2) was calculated using the OPTIC program available in the WIEN package.[62] The loss functions were then obtained taking into account both the anisotropy of the structures as well as relativistic effects.[63] In the OPTIC program, the random-phase approximation is used without the inclusion of local field effects (LFEs).[26] In some cases, the calculation of the macroscopic dielectric constant neglecting off- diagonal terms in the dielectric matrix inversion modifies significantly calculated peak intensities and may induce small energy shifts.[64,65] In particular, they have to be included when highly inhomogeneous electronic distributions are considered.[66] LFEs do, however, decrease with decreasing momentum transfer. For instance, loss functions calculated with and without LFEs for small q values in diamond are almost identical.[67] Since we collected electrons scattered through an on-axis circular aperture, very small momentum transfers contribute the most to the intensity of our experimental spectrum. In our case, LFEs can therefore be neglected with confidence.

We present in Fig. 10 the results for the *AB* and *ZZ* structures compared with an experimental spectrum. The presence of a π plasmon peak around 5 eV in the experimental spectrum confirms the 2D character of the structure. This peak is rather well reproduced by the simulated spectra for the *AB* and *ZZ* structures, which indicates a similarity between these hypothetical structures and that of the experimental compound. The lower $\pi+\sigma$ plasmon peak around 22 eV in the *ZZ* structure, when compared with that of the 27 eV in the *AB* structure, was expected. A plasmon energy may be associated with the density of electrons per volume unit involved in the transitions up to that energy. As the *ZZ* structure is, primarily, obtained from the *AB* structure by removing one C_3N_3 ring out of three (Fig. 6), the number of electrons available for the transitions is reduced. The same observation can be made when examining the plasmon position of amorphous carbon compared to that of graphite.[68] The experimen-

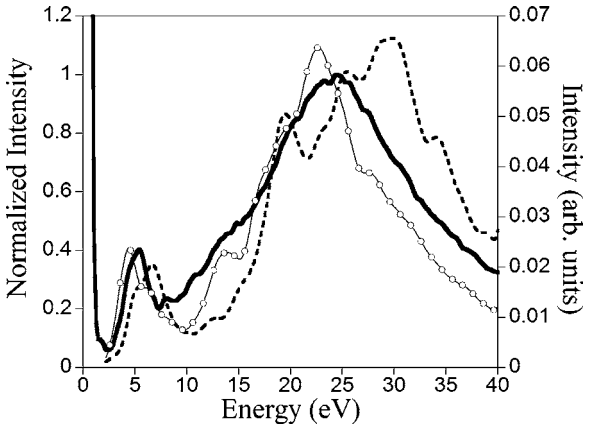

FIG. 10. Comparison of the experimental low-loss spectrum of our sample (thick line) with the *AB* calculation (dashed line) and the *ZZ* structure calculation (line with empty circles).

tal $\pi+\sigma$ plasmon peak is situated between the two calculated ones. This is indicative of a reduced electron density from the pure *AB* structure. The low-energy-loss results are consequently very compatible with an *AB* structure which is defective (missing hexagons) and which is locally similar to the *ZZ* one.

VI. CONCLUSION

From our initial study of reference compounds, we showed that, at least for B, C, and N elements, it was possible to use the non-time-dependent DFT to satisfactorily simulate experimental spectra. However, it is necessary to partition the spectra into two regions: in the low-energy one (0–7 eV above threshold) a full core hole must be considered, whereas a very small one is enough in the region starting approximately 12 ev above threshold. The energy range in between remains poorly described and illustrates the fact that this approach is only an approximation which cannot take into account excitonic effects. In comparing theory and experiment, we also showed the reasonable fit that could be obtained in considering a very simple approach to the lifetime broadening due to the excited electron. The goodness of the fit allows us to apply this approach to an unknown compound made of nitrogen and carbon atoms. In addition to the electronic structure information, EELS could give us the composition of that compound: very close to three carbon atoms for four nitrogen ones. By comparing the experimental spectra at both *K* edges with simulated ones for different possible structures, we identified our compound as being very close to the $(C_3N_3)_2(NH)_3$ lamellar compound or to a very defective hexagonal 2D C_3N_4 (ABA stacking). This determination is particularly important since this latter phase is believed to be remarkably adequate for a transition under high pressure to a 3D C_3N_4 phase. Finally, the theoretical considerations exposed in this paper should make the identification of a possible 3D C_3N_4 phase more reliable.

ACKNOWLEDGMENTS

The computations presented in this work were performed at the "Centre Régional de Calcul Intensif des Pays de la Loire" financed by the French Research Ministry, the "Région Pays de la Loire," and Nantes University.

[1] A. Y. Liu and M. L. Cohen, Science **245**, 841 (1989).
[2] D. M. Teter and R. J. Hemley, Science **271**, 53 (1996).
[3] A. Snis and S. F. Matar, Phys. Rev. B **60**, 10855 (1999); M. Mattesini, S. F. Matar, A. Snis, J. Etourneau, and A. Mavromaras, J. Mater. Chem. **9**, 3151 (1999).
[4] N. Mubumbila, B. Bouchet-Fabre, C. Godon, C. Marhic, B. Angleraud, P-Y. Tessier, and T. Minea, Diamond Relat. Mater. **13**, 1433 (2004).
[5] S. Trasobares, S. P. Gao, O. Stéphan, A. Gloter, C. Colliex, and J. Zhu, Chem. Phys. Lett. **352**, 12 (2002).
[6] A. T. Paxton, A. J. Craven, J. M. Gregg, and D. W. McComb, J. Microsc. **210**, 35 (2003).
[7] M. Kawaguchi and N. Nozaki, Chem. Mater. **7**, 257 (1995).
[8] Z. Zhang, K. Leinenweber, M. Bauer, L. A. J. Garvie, P. F. McMillan, and G. H. Wolf, J. Am. Chem. Soc. **123**, 7788 (2001).
[9] A. C. Ferrari, A. Libassi, B. K. Tanner, V. Stolojan, J. Yuan, L. M. Brown, S. E. Rodil, B. Kleinsorge, and J. Robertson, Phys. Rev. B **62**, 11089 (2000).
[10] R. F. Egerton, *Electron Energy Loss Spectroscopy in the Electron Microscope*, 2nd ed. (Plenum Press, New York, 1996).
[11] M. Varela, S. D. Findlay, A. R. Lupini, H. M. Christen, A. Y. Borisevich, N. Dellby, O. L. Krivanek, P. D. Nellist, M. P. Oxley, L. J. Allen, and S. J. Pennycook, Phys. Rev. Lett. **92**, 095502 (2004).
[12] C. Mitterbauer, G. Kothleitner, W. Grogger, H. Zandbergen, B. Freitag, P. Tiemeijer, and F. Hofer, Ultramicroscopy **96**, 469 (2003).
[13] C. Hébert, J. Luitz, and P. Schattschneider, Micron **34**, 219 (2003).
[14] V. J. Keast, A. J. Scott, R. Brydson, D. B. Williams, and J. Bruley, J. Microsc. **203**, 135 (2001).
[15] A. T. Paxton, M. van Schilfgaarde, M. MacKenzie, and A. J. Craven, J. Phys.: Condens. Matter **12**, 729 (2000).
[16] J. C. Le Bossé, M. Sennour, C. Esnouf, and H. Chermette, Ultramicroscopy **99**, 49 (2004).
[17] C. Mitterbauer, C. Hebert, G. Kothleitner, F. Hofer, P. Schattschneider, and H. W. Zandbergen, Solid State Commun. **130**, 209 (2004).
[18] S. Lazar, C. Hébert, and H. W. Zandbergen, Ultramicroscopy **98**, 249 (2004).
[19] V. J. Keast, M. J. Kappers, and C. J. Humphreys, J. Microsc. **210**, 89 (2003).
[20] O. Stéphan, M. Kociak, L. Henrard, K. Suenaga, A. Gloter, M. Tence, E. Sandre, and C. Colliex, J. Electron Spectrosc. Relat. Phenom. **114**, 209 (2001).
[21] J. T. Titantah, K. Jorissen, and D. Lamoen, Phys. Rev. B **69**,

125406 (2004).
[22] J. B. Neaton, D. A. Muller, and N. W. Ashcroft, Phys. Rev. Lett. **85**, 1298 (2000).
[23] R. Ahuja, P. A. Brühwiler, J. M. Wills, B. Johansson, N. Martensson, and O. Eriksson, Phys. Rev. B **54**, 14396 (1996).
[24] P. E. Batson, Phys. Rev. B **48**, 2608 (1993).
[25] C. Hébert-Souche, P.-H. Louf, P. Blaha, M. Nelhiebel, J. Luitz, P. Schattschneider, K. Schwarz, and B. Jouffrey, Ultramicroscopy **83**, 9 (2000).
[26] G. Onida, L. Reining, and A. Rubio, Rev. Mod. Phys. **74**, 601 (2002).
[27] E. L. Shirley, Phys. Rev. Lett. **80**, 794 (1998).
[28] E. L. Shirley, J. Electron Spectrosc. Relat. Phenom. **136**, 77 (2004).
[29] J. Luitz, M. Maier, C. Hébert, P. Schattscneider, P. Blaha, K. Schwarz, and B. Jouffrey, Eur. Phys. J. B **21**, 363 (2001).
[30] G. Goglio, D. Andrault, S. Courjault, and G. Demazeau, High Press. Res. **22**, 535 (2002).
[31] P. Fallon and C. Walsh, computer code PEELS (University of Cambridge, United Kingdom, 1996).
[32] P. Blaha, K. Schwarz, G. Madsen, D. Kvasnicka, and J. Luitz, Computer code WIEN2K, an augmented plane wave + local orbitals program for calculating crystal properties (Techn. Universität Wien, Austria, 2002).
[33] J. P. Perdew and Y. Wang, Phys. Rev. B **45**, 13244 (1992).
[34] P. Blaha, K. Schwarz, P. Sorantin, and S. B. Trickey, Comput. Phys. Commun. **59**, 399 (1990).
[35] E. Sjöstedt, L. Nordström, and D. J. Singh, Solid State Commun. **114**, 15 (2000).
[36] S. I. Zabinsky, J. J. Rehr, A. Ankudinov, R. C. Albers, and M. J. Eller, Phys. Rev. B **52**, 2995 (1995).
[37] M. P. Seah and W. A. Dench, Surf. Interface Anal. **1**, 2 (1979).
[38] G. Kresse and J. Furthmüller, Comput. Mater. Sci. **6**, 15 (1996); Phys. Rev. B **54**, 11169 (1996).
[39] P. E. Blöchl, Phys. Rev. B **50**, 17953 (1994).
[40] G. Kresse and D. Joubert, Phys. Rev. B **59**, 1758 (1999).
[41] J. P. Perdew, K. Burke, and M. Ernzerhof, Phys. Rev. Lett. **77**, 3865 (1996).
[42] O. Stéphan, P. M. Ajayan, C. Colliex, F. Cyrot-Lackmann, and E. Sandré, Phys. Rev. B **53**, 13824 (1996).
[43] P. A. Brühwiler, A. J. Maxwell, C. Puglia, A. Nilsson, S. Andersson, and N. Martensson, Phys. Rev. Lett. **74**, 614 (1995).
[44] M. Wibbelt, H. Kohl, and P. Kohler-Redlich, Phys. Rev. B **59**, 11739 (1999).
[45] A. Bianconi, M. Dell'Ariccia, A. Gargano, and C. R. Natoli, in *EXAFS and Near Edge Structure*, edited by A. Bianconi, L. Incoccia, and S. Stipcich (Springer-Verlag, Berlin, 1983), p. 57.
[46] F. R. McFeely, S. P. Kowalczyk, L. Ley, R. G. Cavell, R. A. Pollak, and D. A. Shirley, Phys. Rev. B **9**, 5268 (1974).
[47] N. K. Menon and J. Yuan, Ultramicroscopy **78**, 185 (1999).
[48] C. Souche, B. Jouffrey, G. Hug, and M. Nelhiebel, Micron **29**, 419 (1998).
[49] H. R. Daniels, R. Brydson, A. Brown, and B. Rand, Ultramicroscopy **96**, 547 (2003).
[50] B. Jouffrey, P. Schattscneider, and C. Hébert, Ultramicroscopy **102**, 61 (2004).
[51] M. Imamura, K. Shimada, N. Matsubayashi, M. Yumura, K. Uchida, S. Oshima, Y. Kuriki, Y. Yoshimura, T. Sato, and A. Nishijima, Jpn. J. Appl. Phys., Part 2 **33**, L1016 (1994).
[52] D. A. Fischer, R. M. Wentzcovitch, R. G. Carr, A. Continenza, and A. J. Freeman, Phys. Rev. B **44**, 1427 (1991).
[53] C. J. Pickard, M. C. Payne, L. M. Brown, and M. N. Gibbs, in *Electron Microscopy and Analysis Group Conference*, IOP Conf. Proc. No. 147 (IOP, London, 1995), p. 211.
[54] H. Daniels, A. Brown, A. Scoot, T. Nitchells, B. Rand, and R. Brydson, Ultramicroscopy **96**, 523 (2003).
[55] C. Ziethen, O. Schmidt, G. K. L. Marx, G. Schönhense, R. Frömter, J. Gilles, J. Kirschner, C. M. Schneider, and O. Gröning, J. Electron Spectrosc. Relat. Phenom. **107**, 261 (2000).
[56] R. Franke, S. Bender, J. Hormes, A. A. Pavlychev, and N. G. Fominych, Chem. Phys. **216**, 243 (1997).
[57] A. L. Ankudinov, B. Ravel, J. J. Rehr, and S. D. Conradson, Phys. Rev. B **58**, 7565 (1998).
[58] Y. Ma, P. Skytt, N. Wassdahl, P. Glans, D. C. Mancini, J. Guo, and J. Nordgren, Phys. Rev. Lett. **71**, 3725 (1993).
[59] D. R. Hamann and D. A. Muller, Phys. Rev. Lett. **89**, 126404 (2002).
[60] I. Alves, G. Demazeau, B. Tanguy, and F. Weil, Solid State Commun. **109**, 697 (1999).
[61] R. O. Jones and O. Gunnarsson, Rev. Mod. Phys. **61**, 689 (1989).
[62] C. Ambrosch-Draxl, J. A. Majewski, P. Vogl, and G. Leising, Phys. Rev. B **51**, 9668 (1995).
[63] P. Moreau and M.-C. Cheynet, Ultramicroscopy **94**, 293 (2003).
[64] B. Arnaud and M. Alouani, Phys. Rev. B **63**, 085208 (2001).
[65] N. Vast, L. Reining, V. Olevano, P. Schattschneider, and B. Jouffrey, Phys. Rev. Lett. **88**, 037601 (2002).
[66] W. Hanke and L. J. Sham, Phys. Rev. B **12**, 4501 (1975).
[67] S. Waidmann, M. Knupfer, B. Arnold, J. Fink, A. Fleszar, and W. Hanke, Phys. Rev. B **61**, 10149 (2000).
[68] J. T. Titantah and D. Lamoen, Phys. Rev. B **70**, 033101 (2004).